

Resonant inelastic x-ray scattering study of spin-wave excitations in the cuprate parent compound $\text{Ca}_2\text{CuO}_2\text{Cl}_2$

B. W. Lebert,^{1,2} M. P. M. Dean,³ A. Nicolaou,² J. Pellicciari,⁴ M. Dantz,⁴ T. Schmitt,⁴ R. Yu,⁵ M. Azuma,⁵ J.-P. Castellan,^{6,7} H. Miao,³ A. Gauzzi,¹ B. Baptiste,¹ and M. d'Astuto^{1,*}

¹IMPMC-Sorbonne Universités, Université Pierre et Marie Curie, CNRS, IRD, MNHN 4, place Jussieu, 75252 Paris, France

²Synchrotron SOLEIL, L'Orme des Merisiers, Saint-Aubin, 91192 Gif-sur-Yvette Cedex, France

³Department of Condensed Matter Physics and Materials Science, Brookhaven National Laboratory, Upton, New York 11973, USA

⁴Swiss Light Source, Paul Scherrer Institut, CH-5232 Villigen PSI, Switzerland

⁵Materials and Structures Laboratory, Tokyo Institute of Technology, 4259 Nagatsuta, Midori, Yokohama 226-8503, Japan

⁶Laboratoire Léon Brillouin (CEA-CNRS), CEA-Saclay, F-91911 Gif-sur-Yvette, France

⁷Institute for Solid State Physics, Karlsruhe Institute of Technology, D-76021 Karlsruhe, Germany

(Received 28 October 2016; revised manuscript received 7 March 2017; published 7 April 2017)

By means of resonant inelastic x-ray scattering at the Cu L_3 edge, we measured the spin-wave dispersion along (100) and (110) in the undoped cuprate $\text{Ca}_2\text{CuO}_2\text{Cl}_2$. The data yield a reliable estimate of the superexchange parameter $J = 135 \pm 4$ meV using a classical spin-1/2 two-dimensional Heisenberg model with nearest-neighbor interactions and including quantum fluctuations. Including further exchange interactions increases the estimate to $J = 141$ meV. The 40 meV dispersion between the magnetic Brillouin zone boundary points (1/2, 0) and (1/4, 1/4) indicates that next-nearest-neighbor interactions in this compound are intermediate between the values found in La_2CuO_4 and $\text{Sr}_2\text{CuO}_2\text{Cl}_2$. Due to the low- Z elements composing $\text{Ca}_2\text{CuO}_2\text{Cl}_2$, the present results may enable a reliable comparison with the predictions of quantum many-body calculations, which would improve our understanding of the role of magnetic excitations and of electronic correlations in cuprates.

DOI: [10.1103/PhysRevB.95.155110](https://doi.org/10.1103/PhysRevB.95.155110)

I. INTRODUCTION

Magnetic excitations have been intensively studied in high-temperature superconducting (HTS) cuprates for their possible role in the pairing mechanism of these materials [1–4]. Although several studies have already been carried out by means of inelastic neutron scattering (INS) [3] on a number of cuprate compounds, the interpretation of the data remains highly controversial because of the lack of a theoretical understanding of electronic correlations in realistic systems.

Recently, Cu L_3 edge resonant inelastic x-ray scattering (RIXS) [5,6] has emerged as an alternative probe of the above excitations. This technique extends the energy range probed by INS to higher energies [7], and it also offers the advantage of measuring small single crystals. To the best of our knowledge, in HTS cuprates, RIXS has been hitherto employed to complete previous INS studies on well-known compounds. In the case of $\text{La}_{2-x}\text{Sr}_x\text{CuO}_4$, for example, the RIXS results found that magnetic excitations persist up to very high doping levels in regions of the Brillouin zone that are not easily probed by INS [8].

The purpose of the present work is to study by means of RIXS the HTS cuprate parent compound $\text{Ca}_2\text{CuO}_2\text{Cl}_2$ (CCOC), for which INS studies are infeasible because samples are only available as small, hygroscopic single crystals. This parent compound can be doped either with sodium, $\text{Ca}_{2-x}\text{Na}_x\text{CuO}_2\text{Cl}_2$ (Na-CCOC) [9,10], or with vacancies, $\text{Ca}_{2-x}\text{CuO}_2\text{Cl}_2$ [11]. The motivation of our study is the simplicity of their single-layer tetragonal structure and the absence of structural instabilities that often jeopardize the study of more common cuprates, such as the aforementioned $\text{La}_{2-x}\text{Sr}_x\text{CuO}_4$. Moreover, the $\text{Ca}_2\text{CuO}_2\text{Cl}_2$ system is

the only HTS cuprate system composed exclusively of low Z ions, with copper being the heaviest. This is an advantage for standard *ab initio* density-functional-theory calculations, where large Z ions pose problems for pseudopotential optimization. This feature is even more advantageous for advanced theoretical methods suitable to take into account correlation effects, such as quantum Monte Carlo, since they require one to treat accurately the spin-orbit coupling. To circumvent this difficulty, these quantum many-body calculations are mainly applied to systems with light atoms, where relativistic effects are negligible [12–14]. Note that Ref. [14] treats in particular $\text{Ca}_2\text{CuO}_2\text{Cl}_2$, although without separating the different components of the magnetic exchange interaction. In this respect, $\text{Ca}_{2-x}\text{CuO}_2\text{Cl}_2$ and $\text{Ca}_{2-x}\text{Na}_x\text{CuO}_2\text{Cl}_2$ are the most suitable example of such low- Z systems among HTS cuprates. In addition, the superconducting compound $\text{Ca}_{2-x}\text{Na}_x\text{CuO}_2\text{Cl}_2$ has already been studied by means of photoemission and scanning tunneling spectroscopy [9,15,16], therefore a RIXS study is expected to provide further insight into the electronic excitation spectrum. In the present work, by means of RIXS, we study the spin-wave dispersion of $\text{Ca}_2\text{CuO}_2\text{Cl}_2$, the parent compound of the above HTS cuprate, and we extract the superexchange parameter J using two different models.

II. EXPERIMENTAL METHODS

A. Crystal growth and characterization

Single crystals of $\text{Ca}_2\text{CuO}_2\text{Cl}_2$ were grown from CaCO_3 , CuO , and CaCl_2 by solid state reaction, as described in detail elsewhere [10,11]. As shown in Fig. 1, $\text{Ca}_2\text{CuO}_2\text{Cl}_2$ has a tetragonal K_2NiF_4 -type structure ($I4/mmm$) [19] with alternate stacking of $(\text{Ca},\text{Cl})_2$ and CuO_2 layers. The lattice parameters at ambient conditions are $a = b = 3.867\ 35(2)$ Å

*matteo.dastuto@imPMC.upmc.fr

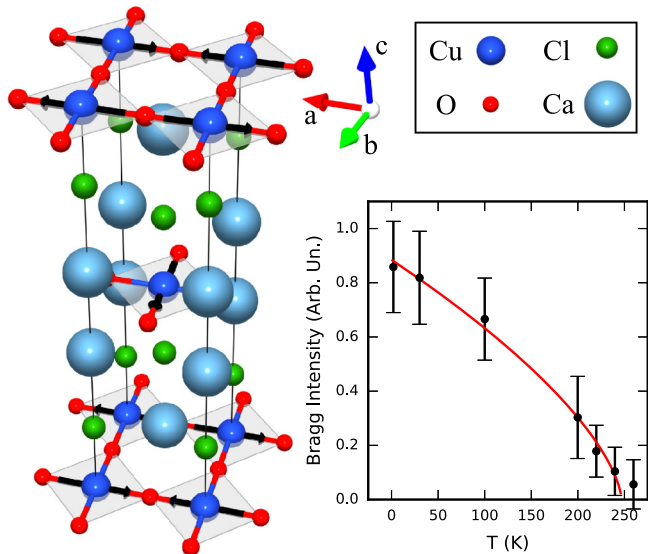


FIG. 1. Top left: Tetragonal crystal structure [17] of $\text{Ca}_2\text{CuO}_2\text{Cl}_2$ [11]. The square coordination of copper with its four nearest-neighbor oxygen ions in the CuO_2 planes is shown. The chlorine ions are located in the apical site above and below the copper. Black arrows indicate one of the possible magnetic structures consistent with neutron-diffraction data [18]. Bottom right: Temperature dependence of the fitted intensity of the averaged Bragg reflections $(\frac{1}{2}, \frac{1}{2}, \frac{5}{2})$ and $(\frac{1}{2}, \frac{1}{2}, \frac{7}{2})$ and a power-law fit (red).

and $c = 15.0412(1) \text{ \AA}$ [10,11]. The crystals are easily cleaved along the ab plane due to the weak ionic bonds between adjacent layers.

The single crystals of ≈ 2 mm width/height and ≈ 0.2 mm thickness were characterized using a commercial Bruker four-circle κ geometry diffractometer. A fixed Mo anode was used and the filtered $K\alpha$ emission was collimated at 0.2 mm (3 mrad). A cryogenic N_2 flux was used to isolate the sample from humidity. The measurements yield unit-cell parameters in agreement with the literature [10,11], and they also enabled us to determine the crystal orientation with respect to visible facets. The samples for RIXS measurements were subsequently glued on the holder with silver epoxy. Finally, ceramic posts were attached with the same epoxy in order to cleave the crystals in vacuum.

$\text{Ca}_2\text{CuO}_2\text{Cl}_2$ is an antiferromagnetic insulator with a Néel temperature of $T_N = 247 \pm 5$ K [18]. To check the magnetic state of the samples, we performed neutron scattering on the 1T spectrometer at Laboratoire Leon-Brillouin using a sample from the same batch used for the RIXS experiment. We measured very weak magnetic reflections at low temperature for $\mathbf{q} = (\frac{1}{2}, \frac{1}{2}, \frac{\ell}{2})$ with $\ell = 2n + 1$ ($n = 0, \dots, 4$), but none for $\ell = 0$, in agreement with Ref. [18]. The temperature dependence of the fitted Bragg intensity [average of the $(\frac{1}{2}, \frac{1}{2}, \frac{5}{2})$ and $(\frac{1}{2}, \frac{1}{2}, \frac{7}{2})$ reflections] is shown in the bottom right of Fig. 1, and a power-law fit finds $T_N = 247 \pm 6$ K.

B. Resonant inelastic x-ray scattering

RIXS measurements at the Cu L_3 edge (930 eV) were performed at the ADDRESS beamline [21,22] of the Swiss Light

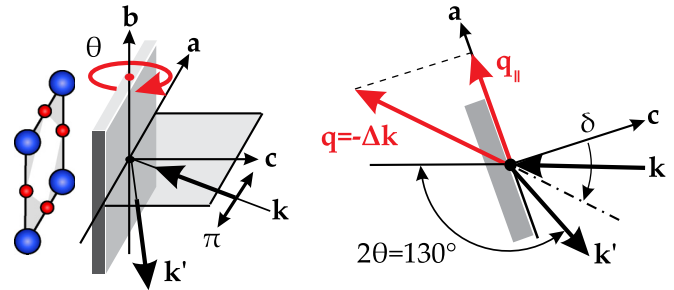


FIG. 2. RIXS geometry for measuring along $\langle 100 \rangle$ with π -polarization and grazing out emission (modified from Ref. [20]). The scattering angle 2θ is defined between the photon momentum of the incoming beam \mathbf{k} and the direction where the analyzer collects the scattered beam \mathbf{k}' . 2θ and the azimuthal angles are fixed, whereas the incident angle can be changed by a rotation, θ , around the b axis. The incident angle defines δ , which is the angle between the sample normal \mathbf{c} and the transferred momentum \mathbf{q} (red arrow), so that $\delta = 0$ in specular reflection. The projection of \mathbf{q} onto the sample's ab plane is denoted q_{\parallel} , which is 0 for $\delta = 0$ and maximal for grazing geometries. Measurements along $\langle 110 \rangle$ are done with the sample rotated 45° around the c axis.

Source using the SAXES spectrometer [23]. The samples were mounted in the ultrahigh-vacuum manipulator cryostat of the experimental station. By applying a force on the aforementioned ceramic posts, the samples were cleaved *in situ* under ultrahigh vacuum and low-temperature conditions to avoid hygroscopic damage of the cleaved surface. Their surface quality was confirmed by x-ray absorption spectroscopy. All spectra presented in this work were taken at 15 K.

The experimental geometry is shown in Fig. 2 and was similar to previous RIXS studies on cuprate parent compounds [6]. We used π -polarized incident x rays and a grazing exit geometry in order to enhance the single magnon spectral weight [7,24–29]. The scattering angle was fixed at $2\theta = 130^\circ$, giving a constant momentum transfer to the sample of $q = 2k \sin(\theta) = 0.85 \text{ \AA}^{-1}$. Although q is fixed, its component in the ab plane, q_{\parallel} , can be changed by rotating the sample about the vertical axis (b axis in Fig. 2). For a given rotation, θ , the deviation from specular reflection is given as $\delta = \theta_{\text{specular}} - \theta$, thus $q_{\parallel} = q \sin(\delta)$. The minimum (maximum) δ used was $+5^\circ$ ($+55^\circ$) corresponding to $q_{\parallel} = +0.07 \text{ \AA}^{-1}$ ($q_{\parallel} = +0.70 \text{ \AA}^{-1}$). Therefore, in terms of reciprocal-lattice units ($2\pi/a$) in the ab plane, we measured q_{\parallel} from (0.05, 0) to (0.43, 0) along $\langle 100 \rangle$ and from (0.03, 0.03) to (0.3, 0.3) along $\langle 110 \rangle$. In other terms (Fig. 6, inset), we measured past the magnetic Brillouin zone along Γ - M , but well short of where thermal neutrons measure at $M = (1/2, 1/2)$. Along Γ - X we measured very close to the first Brillouin zone edge at $X = (1/2, 0)$.

III. RESULTS AND DISCUSSION

The RIXS map of $\text{Ca}_2\text{CuO}_2\text{Cl}_2$ at $q_{\parallel} = (0.34, 0)$ shown in Fig. 3 highlights the resonant behavior of the inelastic features. From lower- to higher-energy loss, one notes a midinfrared peak between 0.1 and 0.6 eV, dd excitations between 1 and 3 eV, and weak charge-transfer excitations at higher energies. A weak fluorescence line is visible at energies above the

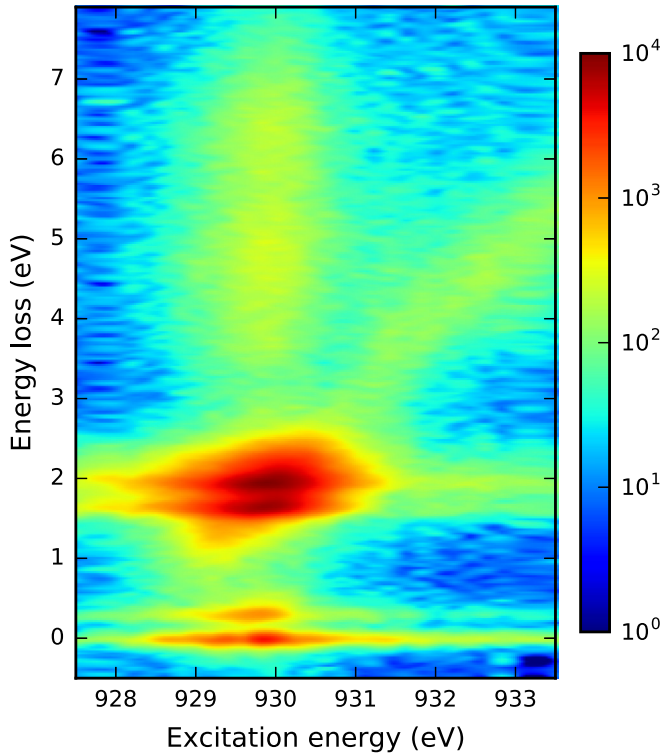


FIG. 3. RIXS map at $\mathbf{q}_{\parallel} = (0.34, 0)$ with π incidence polarization showing the resonant behavior of the magnetic excitations, dd excitations, and charge-transfer excitations. Weak fluorescence is seen at high energy when the system is excited above the Cu L_3 edge threshold. The color map is a logarithmic scale in arbitrary intensity units.

Cu L_3 edge and intersects the dd excitations at resonance. The spectral weight from this fluorescence line at resonance is unknown, but it is likely of the same order as the dd excitations, as evidenced by the diagonal skew of the dd excitations.

Figure 4 shows the RIXS spectra obtained along both directions focusing on the midinfrared energy region, while Fig. 5(a) shows the full energy region for $\delta = +10$ and $+55$. The spectra are normalized to the area of the dd excitations to account for the geometrical changes of the RIXS cross section. There is an expected increase in elastic scattering near specular, i.e., at $(0.09, 0)$ and $(0.06, 0.06)$. However, the elastic line for the sample aligned along $\langle 100 \rangle$ was large for all momentum transfers. These variations are likely due to finite surface quality after cleaving and did not impede accurate fitting.

The midinfrared feature is assigned as a magnon with a higher-energy multimagnon continuum. This assignment was done considering its dispersion (Figs. 4 and 6) and past RIXS results on cuprate parent compounds in this experiment geometry [6,7]. Furthermore, in our case, magnetic excitations are the only excitation in the midinfrared energy region due to the ≈ 2 eV Mott gap. These spin excitations are the focus of our paper and are discussed below.

The apical chlorine in $\text{Ca}_2\text{CuO}_2\text{Cl}_2$ increases the tetragonal distortion much like for $\text{Sr}_2\text{CuO}_2\text{Cl}_2$, therefore based on Ref. [20] we assigned the dd excitation at 1.70 eV to Cu $3d_{xy}$, 1.99 eV to Cu $3d_{xz/yz}$, and higher energies in the shoulder to Cu $3d_{3z^2-r^2}$. The dd excitations were not well fit following the

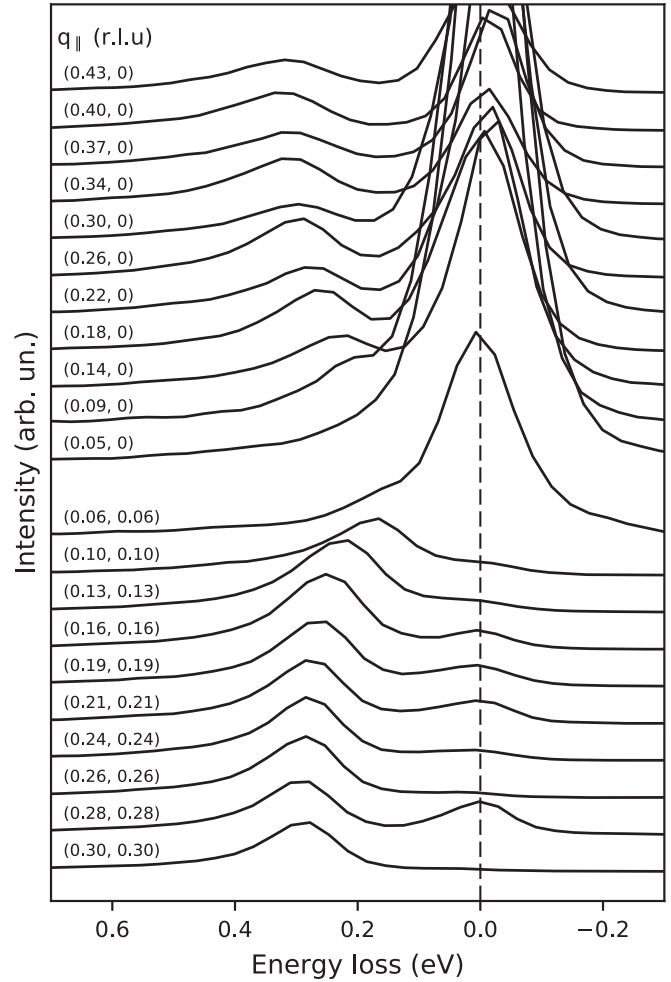


FIG. 4. RIXS spectra showing the dispersion of the magnetic excitations along $\langle 100 \rangle$ (top) and $\langle 110 \rangle$ (bottom). Spectra are normalized by their dd excitations.

technique of Ref. [20], possibly due to fluorescence emission in this energy region or electron-phonon coupling [30].

The broad charge-transfer feature centered around 5.5 eV did not show dispersion or significant intensity variations, in agreement with Cu K edge RIXS [31]. The author of Ref. [31] assigned this feature as transitions to an excited state composed of symmetric contributions of a central Cu $3d_{x^2-y^2}$ orbital and the surrounding O $2p_{\sigma}$ orbitals. Cu K edge RIXS also found a dispersive Mott excitation from 2.35 to 3.06 eV along Γ - X and from 2.34 to 4.14 eV along Γ - M . Therefore, the Mott excitation will fall under the dd excitations for the majority of our momentum transfers, however the Mott excitation at ≈ 3.4 eV for $\mathbf{q}_{\parallel} = (0.3, 0.3)$ is not visible in our results [Fig. 5(a)].

A typical fit of the midinfrared region is shown for $\mathbf{q}_{\parallel} = (0.21, 0.21)$ in Fig. 5(b) and the extracted magnon dispersion is shown in Fig. 6. The resolution function was measured on carbon tape and was well described by a Lorentzian squared function of 130 meV full width at half-maximum. The elastic, phonon, and single magnon contributions were all resolution-limited. The multimagnon excitation continuum was modeled as the resolution function convolved with a step function with subsequent exponential decay toward higher-energy losses.

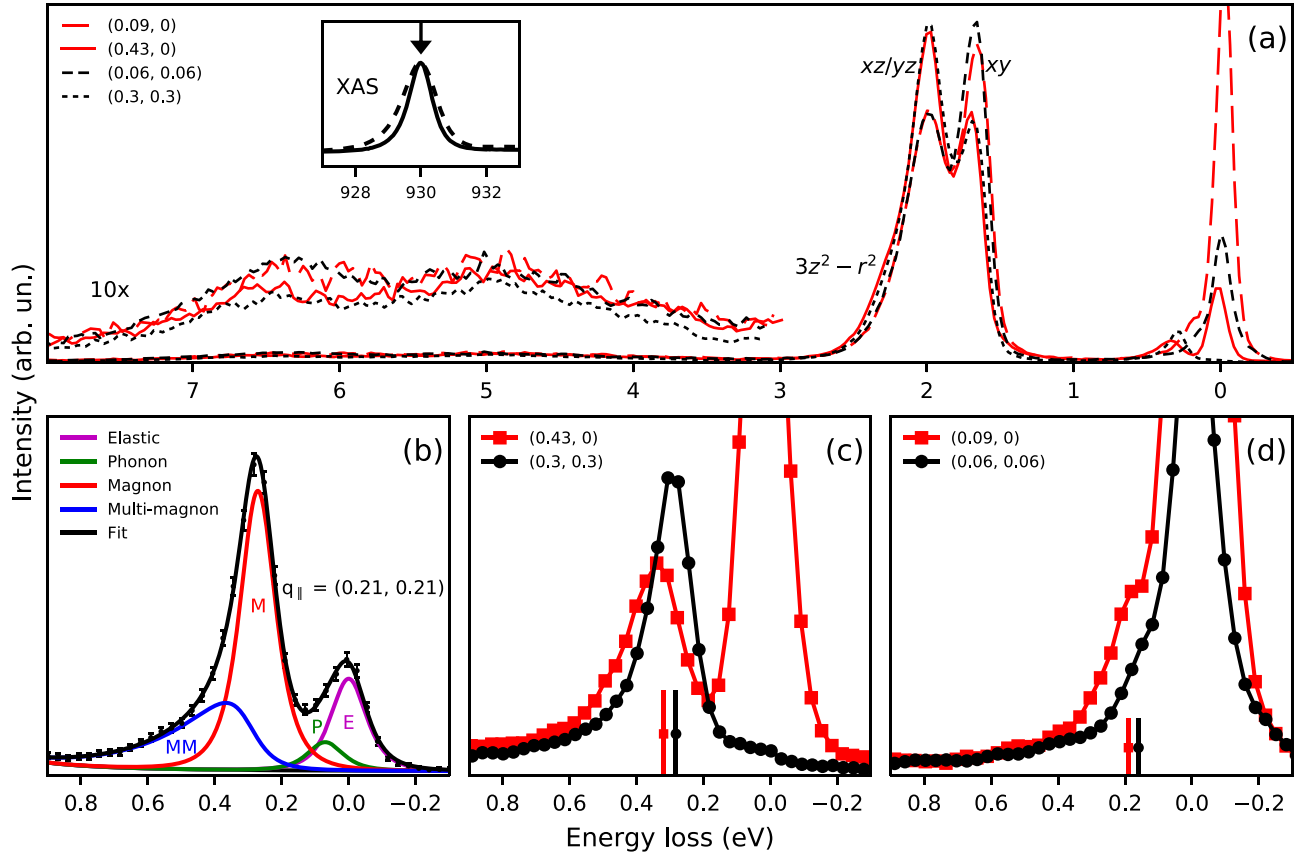


FIG. 5. Cu L_3 RIXS spectra of $\text{Ca}_2\text{CuO}_2\text{Cl}_2$ at different in-plane transferred momentum, \mathbf{q}_{\parallel} , expressed as (h, k) in reciprocal-lattice units. (a) Representative RIXS spectra along $\langle 100 \rangle$ (red) and $\langle 110 \rangle$ (black). All spectra have been normalized to the area of the dd excitations. The midinfrared regions of these spectra are shown in (c,d), where vertical bars represent the energy of a single magnon found by fitting. The inset shows TEY-XAS (solid) and TFY-XAS (dashed), with an arrow indicating incident energy for our RIXS measurements. (b) Example of the fitting procedure at $\mathbf{q}_{\parallel} = (0.21, 0.21)$ shown as a black curve through data points. The elastic (E , magenta), phonon (P , green), and single magnon (M , red) peaks were resolution-limited, and the multimagnon (MM , blue) peak fitting is described in the text.

The background was a Lorentzian tail of the form $y = A(x - x_0)^{-2} + c$. The energy of the phonon contribution is found around 60–70 meV with respect to the elastic, or ~ 15 –17 THz, roughly corresponding to the Debye cutoff frequency ω_D of $\text{Ca}_2\text{CuO}_2\text{Cl}_2$ [32]. The major source of uncertainty for the magnon energy was determining the elastic energy, since the elastic line was irregular for the sample aligned along $\langle 100 \rangle$ and often too weak along $\langle 110 \rangle$. dd excitations in undoped layered cuprates are known to be nondispersive within current experimental accuracy [20], therefore the elastic energy was fixed with respect to the Cu $3d_{xz/yz}$ energy, which was found to be 1985 ± 5 meV from several spectra with well-defined elastic lines.

The experimental and calculated dispersion along the two high-symmetry directions is shown together in Fig. 6. We use a classical $S = 1/2$ 2D Heisenberg model with higher-order coupling to analyze our dispersion. The Hamiltonian is given by [33]

$$\begin{aligned} \mathcal{H} = & J \sum_{\langle i,j \rangle} \mathbf{S}_i \cdot \mathbf{S}_j + J' \sum_{\langle i,i' \rangle} \mathbf{S}_i \cdot \mathbf{S}_{i'} + J'' \sum_{\langle i,i'' \rangle} \mathbf{S}_i \cdot \mathbf{S}_{i''} \\ & + J_c \sum_{\langle i,j,k,l \rangle} \{(\mathbf{S}_i \cdot \mathbf{S}_j)(\mathbf{S}_k \cdot \mathbf{S}_l) + (\mathbf{S}_i \cdot \mathbf{S}_l)(\mathbf{S}_k \cdot \mathbf{S}_j) \\ & - (\mathbf{S}_i \cdot \mathbf{S}_k)(\mathbf{S}_j \cdot \mathbf{S}_l)\}, \end{aligned}$$

where we include first-, second-, and third-nearest-neighbor exchange terms, as well as a ring exchange term (J , J' , J'' , and J_c). Within classic linear spin-wave theory [34,35], this leads to a dispersion relation given by [33] $\hbar\omega_{\mathbf{q}} = 2Z_C(\mathbf{q})\sqrt{A_{\mathbf{q}}^2 - B_{\mathbf{q}}^2}$, where $A_{\mathbf{q}}^2 = J - J_c/2 - (J' - J_c/4)(1 - \nu_h\nu_k) - J''[1 - (\nu_{2h} + \nu_{2k})/2]$, $B_{\mathbf{q}}^2 = (J - J_c/2)(\nu_h + \nu_k)/2$, $\nu_x = \cos(2\pi x)$, and $Z_C(\mathbf{q})$ is a spin renormalization factor [33,36].

As a first approximation, we consider only the first term in the Hamiltonian, which corresponds to only nearest-neighbor exchange. In this isotropic case, the dispersion relation above reduces to $\hbar\omega_{\mathbf{q}} = 2JZ_C\sqrt{1 - [\cos(2\pi h) + \cos(2\pi k)]^2/4}$, where $Z_c = 1.18$ is a constant [36]. The calculation for our data is shown in Fig. 6 as a solid red line, obtained both analytically and using the SPINWAVE code [35], as a check. The energy at the zone boundary peaks at $2JZ_C = 320 \pm 10$ meV, which gives $J = 135 \pm 4$ meV. For La_2CuO_4 and $\text{Sr}_2\text{CuO}_2\text{Cl}_2$, the zone boundary energy is 314 ± 7 and 310 meV, respectively, which corresponds to $J = 133 \pm 3$ and 131 meV, respectively [7,33].

Note the 40 ± 10 meV energy difference along the magnetic Brillouin zone boundary (MBZB) between X and M . This MBZB dispersion is an indication of non-negligible magnetic

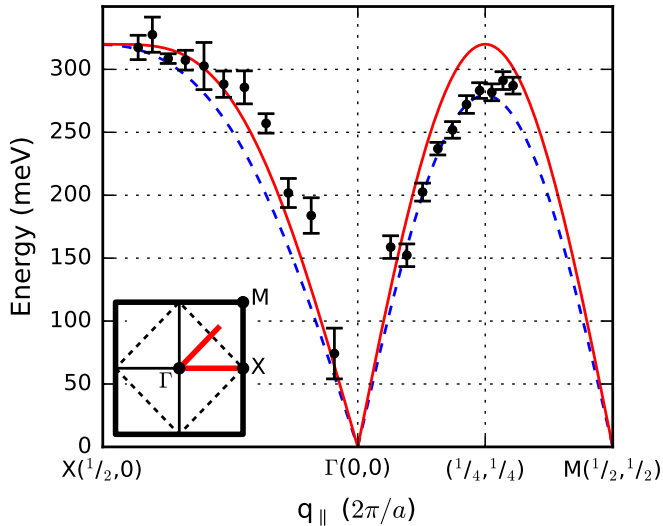


FIG. 6. Dispersion of $\text{Ca}_2\text{CuO}_2\text{Cl}_2$ measured using $\text{Cu } L_3$ RIXS. The red, continuous line is a calculation for a classical spin-1/2 2D Heisenberg model with nearest-neighbor exchange, and the blue, dashed line is a calculation including further exchange terms that is described in the text. Inset: 2D Brillouin zone showing high-symmetry points. The first Brillouin zone boundary is represented by a thick black square, while the magnetic Brillouin zone boundary is represented by a dashed line. The region where we measured is shown as two thick red lines along Γ - X and Γ - M .

interactions beyond nearest neighbors [7,33,37]. Following Ref. [33], we parametrize the above Hamiltonian with a single-band Hubbard model with U , the on-site repulsion, and t , the nearest-neighbor hopping. Expanding the Hubbard Hamiltonian to order t^4 , we find $J = 4t^2/U - 24t^4/U^3$, $J_c = 80t^4/U^3$, and $J' = J'' = 4t^4/U^3$. We assume the spin renormalization is constant, $Z_c(\mathbf{q}) \approx Z_c$, which introduces an error less than the uncertainty of our data [33]. Within this model, it can be shown [38] that the maximum energy at X is given by $E_{\max} = 2Z_c(J - J_c/10)$ and the energy dispersion along the MBZB is given as $\Delta E_{\text{MBZB}} = 3Z_c J_c/5$. We can use our experimental dispersion to fix $E_{\max} = 320$ meV and $\Delta E_{\text{MBZB}} = 40$ meV, which uniquely determines $U = 2.2$ eV and $t = 295$ meV. The corresponding superexchange parameter is $J = 141$ meV, versus $J = 146$ meV for La_2CuO_4 and $J = 144$ meV for $\text{Sr}_2\text{CuO}_2\text{Cl}_2$. The calculated dispersion using these values is shown in Fig. 6 as a dashed blue line. The MBZB dispersion is well fit, however the energy along $\langle 100 \rangle$ is underestimated, indicating the need to include further hopping terms in the Hubbard model [37,39]. Furthermore, our values of U and t are unphysical, even if they are similar to those found in La_2CuO_4 at 10 K using this approach [33] ($U = 2.2$ eV and $t = 300$ meV). They are in disagreement with photoemission results [40], and $U = 7.5t$ is less than the tight-binding bandwidth [39] of $8t$. Inclusion of further hopping terms is beyond the scope of this paper, however they will not fundamentally change the determination of the superexchange parameter J .

The fact that all three cuprates discussed above have a very similar E_{\max} is a bit surprising. The simplistic scaling relation [41] $J \propto d_{\text{NN}}^{-4}$ based on the intraplanar Cu NN distance

would predict a 7% softening of $\text{Ca}_2\text{CuO}_2\text{Cl}_2$ with respect to La_2CuO_4 ($d_{\text{NN}} = 3.803$ Å) [42] and an 11% hardening with respect to $\text{Sr}_2\text{CuO}_2\text{Cl}_2$ ($d_{\text{NN}} = 3.975$ Å) [42].

On the other hand, these three cuprates have different ΔE_{MBZB} , with La_2CuO_4 being smaller (22 ± 10 meV) and $\text{Sr}_2\text{CuO}_2\text{Cl}_2$ being larger (70 meV). With further exchange terms [43] it is found that the dispersion scales as $(t'/t)^2$, where t' is the next-nearest-neighbor hopping. This second hopping term is typically decreased due to apical hybridization [44], therefore we would expect greater dispersion for longer apical bonds lengths. This is indeed the trend we see for these three compounds: $\text{Sr}_2\text{CuO}_2\text{Cl}_2$ (2.8612 Å) > $\text{Ca}_2\text{CuO}_2\text{Cl}_2$ (2.734 Å) > La_2CuO_4 (2.416 Å). If this interpretation is correct, then our assignment of the shoulder in the dd excitations to $\text{Cu } 3d_{3z^2-r^2}$ is likely incorrect since we would then expect $E_{3z^2-r^2}$ for $\text{Ca}_2\text{CuO}_2\text{Cl}_2$ to be less than 1.97 eV ($\text{Sr}_2\text{CuO}_2\text{Cl}_2$) and more than 1.7 eV (La_2CuO_4) [20].

Although Ref. [14] did not report a value of J , the current uncertainty in QMC calculations allows a rough comparison between them and experiment. QMC calculations [12,13] have found $J = 160(13)$ meV for La_2CuO_4 , $J = 140(20)$ meV for CaCuO_2 , and $J = 159(14)$ meV for Ca_2CuO_3 . The value found for La_2CuO_4 is quite different from its experimental value, possibly due to relativistic effects in the La atoms. CaCuO_2 and $\text{Ca}_2\text{CuO}_2\text{Cl}_2$ are both composed of CuO_2 planes with interplanar Ca atoms, however CaCuO_2 lacks any apical ligand. Nonetheless, its calculated value matches quite well our results above, much better than the Cu chain system of Ca_2CuO_3 , which has apical oxygens, emphasizing the important role that the apical ligands play in intraplanar (chain) exchange.

IV. CONCLUSIONS

In conclusion, the present $\text{Cu } L_3$ edge RIXS study enabled us to determine the spin-wave dispersion along the two high-symmetry directions of $\text{Ca}_2\text{CuO}_2\text{Cl}_2$, an undoped antiferromagnetic HTS cuprate parent compound containing only low- Z elements. In a first approximation, the data are explained within a simple $S = 1/2$ 2D Heisenberg model with a nearest-neighbor exchange term $J = 135 \pm 4$ meV, taking into account spin quantum fluctuation renormalization. Including next-nearest-neighbor contributions, our estimate is increased to $J = 141$ meV. To the best of our knowledge, this is the first measurement of the spin-wave dispersion and of its zone-boundary energy in $\text{Ca}_2\text{CuO}_2\text{Cl}_2$, noting that INS experiments are currently infeasible, and two-magnon Raman scattering has not been performed yet. We believe that the present low- Z cuprate $\text{Ca}_2\text{CuO}_2\text{Cl}_2$ is an ideal playground for future quantum many-body theoretical models of HTS cuprates. Our RIXS results combined with the future results of these models will offer a unique comparison between experiment and state-of-the-art theory of correlated electron systems.

ACKNOWLEDGMENTS

The authors acknowledge the Paul Scherrer Institut, Villigen-PSI, Switzerland for provision of synchrotron radiation beamtime at beamline X03MA, "ADRESS" of the

Swiss Light Source, as well as LLB and KIT for providing neutron beamtime on the 1T spectrometer, and we would like to thank Yvan Sidis for his assistance. We are grateful to Jean-Pascal Rueff, Sylvain Petit, and Marco Moretti for fruitful discussions, as well as Lise-Marie Chamoreau from the “Plateforme Diffraction” at IPCM for help in crystallographic orientation. We are very grateful to Sylvain Petit for his help with the SPINWAVE code [35]. B.L. acknowledges financial support from the French state funds managed by the Agence Nationale de la Recherche (ANR) within the “Investissements d’Avenir” programme under reference ANR-11-IDEX-0004-02, and within the framework of the Cluster of Excellence MATISSE led by Sorbonne Université and from the LLB/SOLEIL Ph.D. fellowship program. This material is based upon work supported by the U.S. Department of

Energy, Office of Basic Energy Sciences, Early Career Award Program under Award No. 1047478. Brookhaven National Laboratory was supported by the U.S. Department of Energy, Office of Science, Office of Basic Energy Sciences under Contract No. DE-SC00112704. J.P. and T.S. acknowledge financial support through the Dysenos AG by Kabelwerke Brugg AG Holding, Fachhochschule Nordwestschweiz, and the Paul Scherrer Institut. M.D. acknowledges financial support from the Swiss National Science Foundation within the D-A-CH programme (SNSF Research Grant No. 200021L 141325). The research leading to these results has received funding from the European Community’s Seventh Framework Programme (FP7/2007-2013) under grant agreement n. °312284. This work was written on the collaborative OVERLEAF platform [45].

-
- [1] D. J. Scalapino, *Phys. Rep.* **250**, 329 (1995).
- [2] J. Orenstein and A. J. Millis, *Science* **288**, 468 (2000).
- [3] Y. Sidis, S. Pailhès, B. Keimer, P. Bourges, C. Ulrich, and L. P. Regnault, *Phys. Status Solidi B* **241**, 1204 (2004).
- [4] P. A. Lee, N. Nagaosa, and X.-G. Wen, *Rev. Mod. Phys.* **78**, 17 (2006).
- [5] L. Braicovich, J. van den Brink, V. Bisogni, M. M. Sala, L. J. P. Ament, N. B. Brookes, G. M. De Luca, M. Salluzzo, T. Schmitt, V. N. Strocov *et al.*, *Phys. Rev. Lett.* **104**, 077002 (2010).
- [6] M. P. M. Dean, *J. Magn. Magn. Mater.* **376**, 3 (2015).
- [7] M. Guarise, B. Dalla Piazza, M. Moretti Sala, G. Ghiringhelli, L. Braicovich, H. Berger, J. N. Hancock, D. van der Marel, T. Schmitt, V. N. Strocov *et al.*, *Phys. Rev. Lett.* **105**, 157006 (2010).
- [8] M. P. M. Dean, G. Dellea, R. S. Springell, F. Yakhov-Harris, K. Kummer, N. B. Brookes, X. Liu, Y.-J. Sun, J. Strle, T. Schmitt *et al.*, *Nat. Mater.* **12**, 1019 (2013). D. Meyers, H. Miao, A. C. Walters, V. Bisogni, R. S. Springell, M. d’Astuto, M. Dantz, J. Pellicciari, H. Y. Huang, J. Okamoto *et al.*, *Phys. Rev. B* **95**, 075139 (2017).
- [9] Z. Hiroi, N. Kobayashi, and M. Takano, *Nature (London)* **371**, 139 (2002).
- [10] Y. Kohsaka, M. Azuma, I. Yamada, T. Sasagawa, T. Hanaguri, M. Takano, and H. Takagi, *J. Am. Chem. Soc.* **124**, 12275 (2002).
- [11] I. Yamada, A. A. Belik, M. Azuma, S. Harjo, T. Kamiyama, Y. Shimakawa, and M. Takano, *Phys. Rev. B* **72**, 224503 (2005).
- [12] K. Foyevtsova, J. T. Krogel, J. Kim, P. R. C. Kent, E. Dagotto, and F. A. Reboredo, *Phys. Rev. X* **4**, 031003 (2014).
- [13] L. K. Wagner and P. Abbamonte, *Phys. Rev. B* **90**, 125129 (2014).
- [14] L. K. Wagner, *Phys. Rev. B* **92**, 161116 (2015).
- [15] K. M. Shen, F. Ronning, D. H. Lu, F. Baumberger, N. J. C. Ingle, W. S. Lee, W. Meevasana, Y. Kohsaka, M. Azuma, M. Takano *et al.*, *Science* **307**, 901 (2005).
- [16] T. Hanaguri, C. Lupien, Y. Kohsaka, D.-H. Lee, M. Azuma, M. Takano, H. Takagi, and J. C. Davis, *Nature (London)* **430**, 1001 (2004).
- [17] K. Momma and F. Izumi, *J. Appl. Crystallogr.* **41**, 653 (2008).
- [18] D. Vaknin, L. L. Miller, and J. L. Zarestky, *Phys. Rev. B* **56**, 8351 (1997).
- [19] H. Müller-Buschbaum, *Angewand. Chem. Int. Ed. Engl.* **16**, 674 (1977).
- [20] M. Moretti Sala, V. Bisogni, C. Aruta, G. Balestrino, H. Berger, N. B. Brookes, G. M. de Luca, D. D. Castro, M. Grioni, M. Guarise *et al.*, *New J. Phys.* **13**, 043026 (2011).
- [21] V. N. Strocov, T. Schmitt, U. Flechsig, T. Schmidt, A. Imhof, Q. Chen, J. Raabe, R. Betemps, D. Zimoch, J. Krempasky *et al.*, *J. Synch. Radiat.* **17**, 631 (2010).
- [22] T. Schmitt, V. N. Strocov, K.-J. Zhou, J. Schlappa, C. Monney, U. Flechsig, and L. Patthey, *J. Electron Spectrosc. Relat. Phenom.* **188**, 38 (2013).
- [23] G. Ghiringhelli, A. Piazzalunga, C. Dallera, G. Trezzi, L. Braicovich, T. Schmitt, V. N. Strocov, R. Betemps, L. Patthey, X. Wang *et al.*, *Rev. Sci. Instrum.* **77**, 113108 (2006).
- [24] L. J. P. Ament, G. Ghiringhelli, M. M. Sala, L. Braicovich, and J. van den Brink, *Phys. Rev. Lett.* **103**, 117003 (2009).
- [25] M. W. Haverkort, *Phys. Rev. Lett.* **105**, 167404 (2010).
- [26] J.-i. Igarashi and T. Nagao, *Phys. Rev. B* **85**, 064422 (2012).
- [27] M. Le Tacon, G. Ghiringhelli, J. Chaloupka, M. M. Sala, V. Hinkov, M. W. Haverkort, M. Minola, M. Bakr, K. J. Zhou, S. Blanco-Canosa *et al.*, *Nat. Phys.* **7**, 725 (2011).
- [28] L. Braicovich, M. M. Sala, L. J. P. Ament, V. Bisogni, M. Minola, G. Balestrino, D. D. Castro, G. M. D. Luca, M. Salluzzo, G. Ghiringhelli *et al.*, *Phys. Rev. B* **81**, 174533 (2010).
- [29] M. P. M. Dean, A. J. A. James, R. S. Springell, X. Liu, C. Monney, K. J. Zhou, R. M. Konik, J. S. Wen, Z. J. Xu, G. D. Gu *et al.*, *Phys. Rev. Lett.* **110**, 147001 (2013).
- [30] J. J. Lee, B. Moritz, W. S. Lee, M. Yi, C. J. Jia, A. P. Sorini, K. Kudo, Y. Koike, K. J. Zhou, C. Monney *et al.*, *Phys. Rev. B* **89**, 041104 (2014).
- [31] M. Z. Hasan, E. D. Isaacs, Z.-X. Shen, L. L. Miller, K. Tsutsui, T. Tohyama, and S. Maekawa, *Science* **288**, 1811 (2000).
- [32] M. d’Astuto, I. Yamada, P. Giura, L. Paulatto, A. Gauzzi, M. Hoesch, M. Krisch, M. Azuma, and M. Takano, *Phys. Rev. B* **88**, 014522 (2013).

- [33] R. Coldea, S. M. Hayden, G. Aeppli, T. G. Perring, C. D. Frost, T. E. Mason, S.-W. Cheong, and Z. Fisk, *Phys. Rev. Lett.* **86**, 5377 (2001).
- [34] A. Chubukov, E. Gagliano, and C. Balseiro, *Phys. Rev. B* **45**, 7889 (1992).
- [35] S. Petit, in *Electronic Structure, Magnetism and Phonons, JDN 18—Neutrons et Simulations*, edited by N. M. M. Johnson and M. Plazanet (EDP Sciences, Les Ulis, 2011), Vol. 12, pp. 105–121.
- [36] R. R. P. Singh, *Phys. Rev. B* **39**, 9760 (1989).
- [37] B. Dalla Piazza, M. Mourigal, M. Guarise, H. Berger, T. Schmitt, K. J. Zhou, M. Grioni, and H. M. Rønnow, *Phys. Rev. B* **85**, 100508 (2012).
- [38] Y. Y. Peng, G. Dellea, M. Minola, M. Conni, A. Amorese, D. Di Castro, G. M. De Luca, K. Kummer, M. Salluzzo, X. Sun *et al.*, [arXiv:1609.05405](https://arxiv.org/abs/1609.05405).
- [39] J.-Y. P. Delannoy, M. J. P. Gingras, P. C. W. Holdsworth, and A.-M. S. Tremblay, *Phys. Rev. B* **79**, 235130 (2009).
- [40] F. Ronning, C. Kim, D. L. Feng, D. S. Marshall, A. G. Loeser, L. L. Miller, J. N. Eckstein, I. Bozovic, and Z.-X. Shen, *Science* **282**, 2067 (1998).
- [41] W. Harrison, *Electronic Structure and the Properties of Solids: The Physics of the Chemical Bond* (Dover, New York, 1989).
- [42] D. Vaknin, S. K. Sinha, C. Stassis, L. L. Miller, and D. C. Johnston, *Phys. Rev. B* **41**, 1926 (1990).
- [43] O. Ivashko, N. E. Shaik, X. Lu, C. G. Fatuzzo, M. Dantz, P. G. Freeman, D. E. McNally, D. Destraz, N. B. Christensen, T. Kurosawa *et al.*, [arXiv:1702.02782](https://arxiv.org/abs/1702.02782) (cond-mat.supr-con).
- [44] E. Pavarini, I. Dasgupta, T. Saha-Dasgupta, O. Jepsen, and O. K. Andersen, *Phys. Rev. Lett.* **87**, 047003 (2001).
- [45] www.overleaf.com.